SILICON NITRIDE MEMBRANES FOR FILTRATION AND SEPARATION

Paul Galambos*, Kevin Zavadil, Randy Shul, Christi Gober Willison, and Sam Miller
of Sandia National Labs, PO Box 5800, MS 1080, Albuquerque NM 87185-1080
http://www.mdl.sandia.gov/Micromachine, *(505)844-1542, FAX (505)844-2991,
pcgalam@sandia.gov

Abstract

Semi-Permeable silicon nitride membranes have been developed using a Bosch[1] etch process followed by a reactive ion etch (RIE) process. These membranes were observed to allow air but not water to pass through them into surface micromachined, silicon nitride microfluidic channels. Membranes with this property have potential use in microfluidic systems as gas bubble traps and vents, filters to remove particles and gas partitioning membranes. Membrane permeation was measured as 1.6 x 10^{-8} $mol / m^2 Pa\ s$ of helium for inline membranes at the entrance and exit of the silicon nitride microfluidic channels.

Keywords: Microfluidics, semi-permeable silicon nitride membrane

1. Introduction

Microfluidic systems have a broad range of potential applications, including applications involving biological fluids and complex chemical samples[7]. An important fluid-handling requirement for such complex samples is constituent separation[6]. Separation of chemical constituents is required for both chemical analysis and synthesis. Separation of interfering constituents is required before accurate concentration measurement of the constituent of interest in a fluid sample can be accomplished. In chemical synthesis the constituents of interest may need to be separated from background constituents that could effect the controlled chemical processing in a reactor. Similarly when dealing with biological materials fluid constituents must also be separated prior to analysis, synthesis or other use. For instance, cells may need to be removed (e.g. centrifugation), or genetic material may need to be taken out of cells (e.g. licing).

In microfluidic systems additional separation issues become important. During the introduction of a fluid sample into a microfluidic system contaminants can also be introduced. These contaminants include particles too large for a microchannel in the system and air bubbles (for liquid flows), as well as small amounts of dust or excess air (unwanted sample dilution). Ideally these contaminants should all be removed. At least the large particles and air bubbles (for liquid flows) must be removed before further sample processing.

Eliminating larger particles or air bubbles may be accomplished using an inline membrane. Ideally the filtering membrane would be contained in the microfluidic system and manufactured using the same techniques used to create the microfluidic system. This would allow easy integration of the filtering systems with other systems for use at intermediate steps during chemical processing (such as in an on-chip chemical synthesis). The membrane could be cleaned using backwash or the entire disposable system could be thrown away after sufficient membrane fouling has occurred.

The filtering membrane would have different properties for different applications. For instance one may be interested in a membrane that allows liquid to pass with only particles below a certain size. Several microfabricated filters of this type have been developed. An “H-filter” which separates constituents based on differences in their diffusion coefficients[2] is an example of a membrane-less filter that can accomplish this objective. This type of filter can separate constituents over a continuous particle size range with some

level of impurity and sample dilution. In some sense this is an active filter because the flow rates into the two input legs of the "H" must be controlled to achieve the desired partitioning and to account for differences in viscosity between the sample and dilution streams.

More typical are passive microfabricated membrane particle filters such as those produced using sacrificial oxide removal[4], silicon or silicon nitride micromachining[3,15], or deposition of membrane material[13,14]. These devices typically filter out particles in the microfiltration regime (approximate pore size 50 nm to 5 microns). For even smaller pore sizes one would probably have to pattern the pores through such membranes by methods other than photolithography.

We have developed a microfabricated membrane filter that operates on a size range below the microfiltration regime. The membrane is permeable to gas but not to liquid. This type of membrane is typically not a porous membrane but rather a pervaporation membrane[8]. A pervaporation membrane could be used in microfluidic systems for air bubble removal, separation of different gases, determination of gas concentration in liquid samples, or the controlled addition of gas into liquid samples. This paper will describe the fabrication of these membranes and attempt to characterize them through observation and permeability measurements.

2. Fabrication

The semi-permeable membranes were discovered by serendipity during the process of etching through from the back side of a wafer to create fluid connections to surface micromachined silicon nitride channels on the front of the wafer. The silicon nitride channels were previously fabricated in a surface micromachining process described elsewhere[5]. During the final step of their fabrication the etch release holes for these channels were sealed in a vacuum process. Therefore the covers of the channels were pulled down until they contacted the bottoms of the channels under the force caused by the pressure difference of approximately 1 atm between the outside and inside of the channels. This collapsed channel condition is shown in Fig. 1. The rings in the figure are interference fringes caused by light reflecting off the bottom of the channels and alternately interfering with and enforcing the light reflecting off the top of the channel covers. In the center of the channels the covers are touching the bottom of the channel. Six fringes are visible in Fig. 1. Each fringe corresponds to a channel cover deflection of $\lambda/2$ or approximately 0.3 μm (300 nm) for visible light. The total deflection at the center of the channel is therefore approximately 1.8 μm, which is the total depth of the channel. The channel covers are touching the bottom of the channel in the center region of the channel.

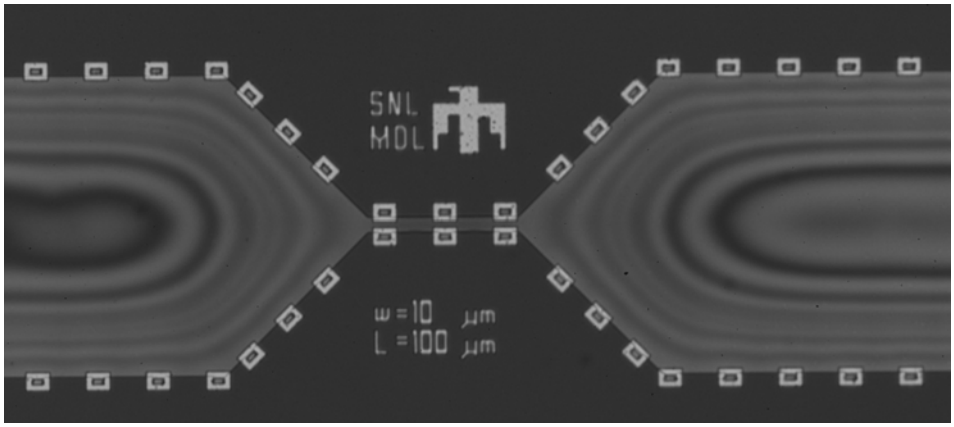

Figure 1. Collapsed Channel. Interference fringes indicate that the top of the channel is collapsed and is touching the bottom of the channel.

These channels (Fig. 1) were post processed to provide fluid entry ports at each end of the channel. A mask with alignment features and 200 micron holes was used to pattern the back of the wafers with entry port holes. Then a Bosch etch process[1] was used to etch these holes through the wafer until they intersected the channel ends on the bottom of the channels. The Bosch process is a DRIE (Deep Reactive Ion Etch) process resulting in anisotropic profiles at room temperature. The process relies on an iterative deposition/etch cycle in which a polymer etch inhibitor is conformally deposited over the silicon wafer during the deposition cycle. During the etch cycle the polymer film is preferentially sputtered from the bottom of the etch via due to the acceleration of ions perpendicular to the surface of the wafer. As a result a deep vertical walled via is etched through the wafer. The Bosch etch stopped on the silicon nitride layer at the bottom of the channels because the etch selectively attacks the silicon much more rapidly than the silicon nitride. At this point the channels were still collapsed as shown in Fig. 1, indicating that the Bosch etch did not break through the silicon nitride membrane to allow air pressure to equalize between the inside and outside of the channels.

One additional process step was required to allow air into the channels and equalize pressure between the inside and outside of the channels. A Plasma-Therm RIE was applied for 8 minutes through the Bosch etched holes. The etch was accomplished using a Plasma-Therm parallel plate RIE etch system (Benchtop) under conditions of: 8.5 *sccm* Ar, 2.5 *sccm* SF_6 , and 2.5 *sccm* CHF_3 at 15 *mTorr* and 150 *W* of power. At the end of 8 minutes the channels were no longer collapsed as indicated by disappearance of the interference fringes - see Fig. 2. Therefore the membrane was shown to be permeable to air after this processing step. We also attempted to break through the membranes using additional exposure time in the Bosch process. However we did not control this exposure time precisely enough and entirely removed the membranes at the channel entry and exit ports.

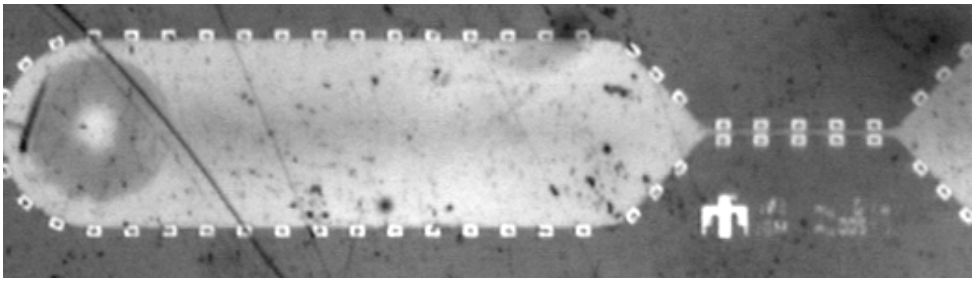

Figure 2. After Bosch and RIE Etch. The membrane is no longer collapsed. The pressure inside and outside of the channel have equalized at atmospheric pressure, indicating that the membranes are permeable to air.

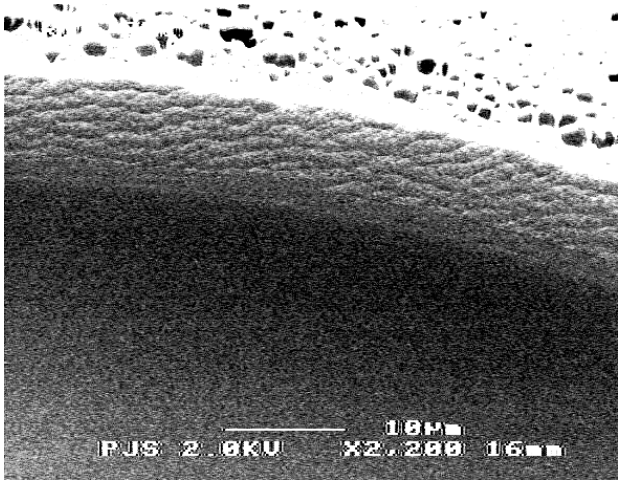

Figure 3. SEM of Membrane after 8 minute RIE etch. The membrane is the darker gray at the bottom.

An SEM (Scanning Electron Micrograph) of the membrane after the 8 minute RIE is shown in Fig. 3. The side of the circular Bosch etched via is shown as the very light porous region in the top portion of the figure. The membrane is the darker gray region in the lower portion of the figure. The surface roughness of the membrane has been increased near the side of the Bosch via (Fig. 3). There also appears to be a radial crack around the membrane separating the rougher portion of the membrane near the via walls with the smoother center portion of the membrane.

3. Observations

These observations were made on silicon nitride channels with bottom membranes exposed to an 8 min RIE overetch. After the processing steps described in the previous section it was reasonable to assume that the bottom of the channel had been removed at each end and that fluids would now flow freely into and out of the channels. This proved, however, not to be the case. Using a syringe we attempted to push water into one end of the channel. Significant deflection of a bottom of channel membrane was observed through interference fringes developed at the entry port when pressure was applied to the membrane using the syringe. The deflection was large enough to cause the bottom membrane to run into the top membrane (approximately 2 μm away) and deflect it. During this deflection process the membranes remained intact. A cyclic application of this force (approximately 10 cycles) caused the membranes to break. When the bottom channel membrane broke the top channel membrane almost invariably broke also. Although in one or two cases the top membrane remained intact when the bottom membrane broke allowing water to enter the microfluidic channels.

The pressure due to the application of thumb force to the syringe plunger can be estimated as follows. Assume ones thumb can apply 50 N of force – equivalent to lifting approximately 10 lb_f. This force is applied over the syringe piston face area resulting in a pressure felt throughout the fluid in the syringe, and therefore at the face of the membrane. The syringe piston face area is approximately 2 x 10^{-5} m^2. Therefore a pressure of approximately 50 N / 2 x 10^{-5} m^2 = 2.5 x 10^6 N/m^2 or approximately 25 atm was applied using the syringe. The membrane withstood this load, but failed when this load was applied cyclically (10 times at approximately 1 Hz).

No water entered the channels during the load application (non-cyclic load application), indicating that the membrane was impervious to water even though air flowed through it. A rapid push of air in a syringe through the membrane caused some membrane deflection, though significantly less than occurred with water in the syringe.

The membrane was left exposed to water, but not under load, for approximately 12 hours (overnight). After 12 hours water was observed inside the channel, indicating condensation in the channel. Either water vapor had passed through the membrane and condensed on the inside of the channel or very slow transport of liquid water had occurred. The water drops were observed downstream from the channel entrance rather than at the entrance membrane.

4. Permeation Measurements

In an effort to quantify gas flow through the membranes, permeation measurements were made on several sets of membranes. Measurements were made of helium permeation for membranes with 8 minutes of RIE overetch (the value at which the channel membranes became permeable to air), 4 minutes of RIE overetch, and 12 minutes of RIE overetch. Helium permeation measurements were also made on membranes with 11, 22, and 33 minutes of overetch using the Bosch process. Overetch refers to etching after the Bosch process has been used to fully expose the silicon nitride membranes. The overetch was applied directly to the membranes, that were 400 μm in diameter for the for the membrane.

4.1 Experimental method

Gas permeability through a membrane can be measured using a simple pressure drop measurement. With this method, a membrane is mounted in a leak tight fixture that separates two independently pumped

vacuum chambers. Dry, ultrahigh purity helium is introduced into one of the chambers, designated the inlet side, and its pressure is monitored (P_i). Outlet pressure (P_o) is monitored in the second chamber, designated the outlet side, using a considerably higher sensitivity measurement technique. A volumetric flow rate per unit membrane area (areal conductance, C_a) can be calculated as follows:

$$C_a = \frac{S_{He}}{(P_i / P_o - 1) \times A}, \text{ Lcm}^{-2}\text{s}^{-1}$$

S_{He} is the pumping speed (L/s) for He of the outlet side chamber and A is the total membrane area. The permeability of the film (IUPAC convention, 1) is obtained by normalizing C_a with the universal gas constant (R, $8.23\text{x}10^{-2}$ $\text{atmLmol}^{-1}\text{K}^{-1}$) and temperature (K). MKS units are preferred[10], requiring a conversion of area to m^2 and pressure to Pa, resulting in:

$$P = \frac{C_a \times 1x10^4}{8.23x10^{-2} \times 1.01x10^5 \times T}, \text{ mol m}^{-2}\text{Pa}^{-1}\text{s}^{-1}$$

The requirements for measuring ultra-low permeability values at low pressure differences and on small area membranes includes high quality vacuum, high sensitivity and stable pressure transducers and a very low sample mount leak rate. We achieve these conditions by using a single vacuum chamber with the sample mounted on the gate of an ultrahigh vacuum compatible valve positioned within the chamber. The inlet and outlet chambers are pumped with a 40 and a 400 Ls^{-1} turbomolecular pump, respectively, when the gate is closed. The inlet chamber pressure is measured using two capacitance diaphragm gauges that are calibrated on the apparatus using a spinning rotor gauge (MKS SRG-2) as a transfer standard (NIST traceable calibration). The outlet chamber pressure is measured using a N_2 calibrated Granville-Phillips Stabil-Ion gauge (NIST traceable calibration). The combination of the ion and spinning rotor gauges allows for the determination of a relative ionization cross-section for He, resulting in a He sensitivity factor of 0.153±0.001 for our ion gauge. Previous measurements of He flow through a 400 micron hole ultrasonically bored into a 100 micron Si wafer yield an outlet chamber pumping speed of 104.2±0.7 Ls^{-1}. Outlet chamber pressures typically sits at $1\text{x}10^{-8}$ to $5\text{x}10^{-9}$ torr at the start of the permeation tests. This level of vacuum provides a lower limit of detection for a pressure ratio difference at 1000 torr of $2{:}10^{13}$ to $2{:}10^{14}$ providing very high sensitivity. Wafer coupons containing the membranes are adhered to a bored aluminum disk, which is o-ring sealed to gate valve seat. Coupons were mounted to allow for a maximum number of films to be tested simultaneously, with numbers ranging from 1 to 6. Membranes were individually examined using optical microscopy to determine which films remained intact and were suitable for permeation testing. A vacuum grade adhesive (Torr-Seal) is used on the coupon. This sealant is slightly permeable to He and this permeability is what actually determines the ultimate sensitivity of this approach.

4.2 Results of permeation measurement

Intrinsic permeability is transport through a porous structure that is generated during deposition or etching rather than by post processing conditions (e.g. high pressure). Ion etched SiN_x films show no intrinsic permeability to He above a value of $7\text{x}10^{-11}$ $\text{mols}^{-1}\text{m}^{-2}\text{Pa}^{-1}$. This conclusion is supported by the permeability data presented in Figure 4 for a series of timed Bosch over-etches running from 11 to 33 minutes. The inlet He pressure was ramped from less than 0.1 torr up to 1000 torr for these measurements. We find no measurable outlet pressure rise resulting in a nearly linear permeability decrease with inlet pressure up to 200 torr. At 260 torr, the 33 min film shows a permeability increase, while the 11 and 22 min films show no increase up to pressures of 1000 torr.

The observed permeability for the 33 min film is the result of pressure induced structural defects in the film. The 33 min data shown in Fig. 4 is actually the second trial from two separate experiments. Comparison of this data with that of the first trial shows a significant shift in detected permeation to lower pressures and higher permeability values for the second trial (see Figure 5).

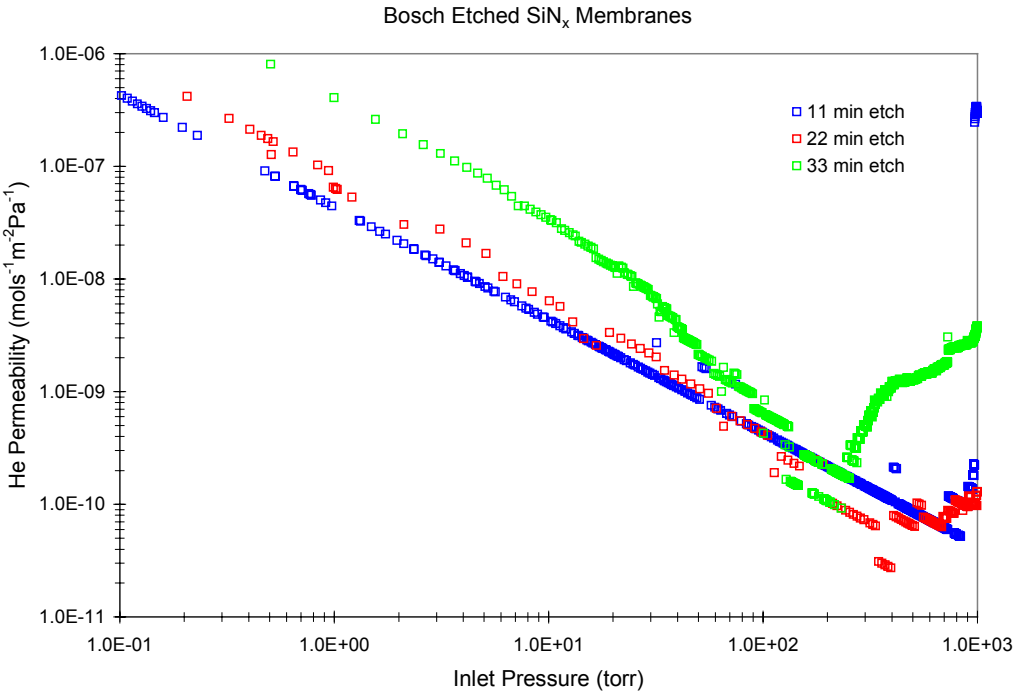

Figure 4: Variation in Bosch Etched SiN_x Film Permeability with Inlet Pressure.

We conclude that this trend to lower pressure transport is the result of pressure induced defects in the film, like micro-fractures. The low and nearly constant value of permeability observed for the 33 min film over the 400 to 700 torr range indicates that film damage is limited to a dimension that supports molecular flow. The mean free path of He at experimental temperatures and 700 torr limits the defect structure to an average cross sectional dimension of less than 150 nm. Further evidence of changes in film transport properties are found in the near 1000 torr response of the 11 min film shown in Figure 5. The 10^3 jump in permeability observed for this film at 1000 torr is evidence of rapid film failure at the highest pressures used.

Figure 6 shows permeation test results of a series of films etched using an alternate plasma chemistry at varying over-etching times. The 4 min etched film shows no detectable permeability for pressures up to 1000 torr. The response of the 12 min film is similar to the 33 min Bosch etched films and may signal some initial film permeability. We observe a permeability value of 1.6×10^{-8} for the 8 min film over a pressure range of 1 to 1000 torr. We estimate the average defect cross sectional parameter to be less than 100 nm. The origin of the permeability decrease at 1000 torr is unclear. We can rule out the possibility of transition flow with some slip flow as a possible source because the measured decrease is a factor of 2 rather than the expected less than 10% value[9,12]. The data of Figure 6 shows no clear correlation between over-etch time and film permeability. The permeability increase observed at high pressure for most of these films is the result of He permeation through the Torr-Seal adhesive used to mount the wafer. This conclusion is best supported by looking at the time-dependent response of each of these films at a constant, high pressure.

We applied a rapid 1000 torr pressure step to the inlet side of the membrane and monitored how long it took to observe a permeability change. The time for gas transport through a pore depends on the size of the pore. In the molecular flow regime (mean free path less than the pore diameter), the pore size dictates the effective diffusion coefficient of a gas molecule along the length of the pore. For a micro-crack, characterized by a width significantly smaller than the thickness of the film, the He transit time will be proportional to the square of the film thickness and inversely proportional to the crack width[11].

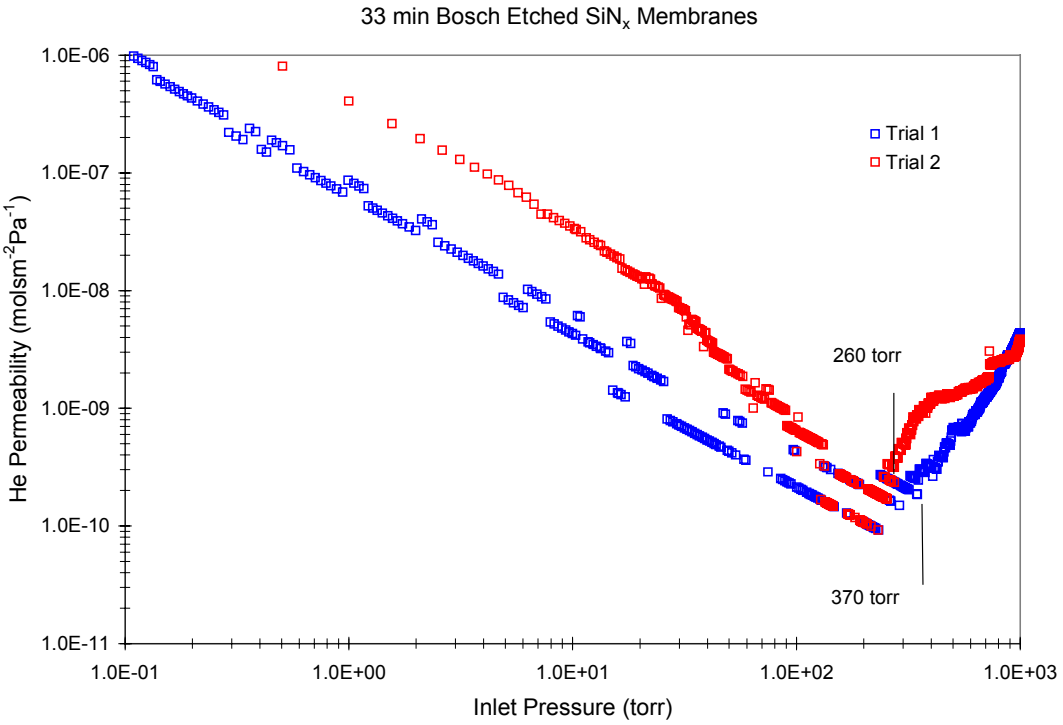

Figure 5: Time Variation in Permeability Response of 33 min Bosch Etched SiN_x Film

Calculation of a transit time for a 1 nm crack through a 1 μm film yields a value less than 1 μsec. The permeability response curves in Figures 7 and 8 show that the 8 min RIE etched and the 33 min Bosch etched films respond instantaneously to the pressure step, indicating that He transport is occurring through porous structure in these films. With the exception of the 11 min Bosch etched film, all other films show a 450 sec delay time followed by a gradual rise in permeability. We find an equivalent length induction time for a solid Si wafer fragment using an identical mounting procedure. We conclude that this induction period is related to the time required for He diffusion through the adhesive. The fact that intrinsic permeability is not detected in some films establishes an upper limit of permeation. We summarize the results in Table 1.

The 11 min Bosch etched film shows evidence for reversible changes in permeation. The ramped pressure measurement was conducted first followed by the pulse experiment. The ramped experiment produced a sudden increase in permeability to $3x10^{-7}$ $mols^{-1}m^{-2}Pa^{-1}$ at 1000 torr. Evacuation of the inlet chamber followed by a 1000 torr step yields an initial permeability of $7x10^{-11}$ followed by a series of instantaneous increases to $3.6x10^{-7}$, $1.4x10^{-6}$, $2.6x10^{-6}$, $4.8x10^{-6}$ and finally $6.3x10^{-6}$ $mols^{-1}m^{-2}Pa^{-1}$. It is possible that this response is due to mechanical stress in the film increasing the width of micro-cracks with film flexure. No further measurements were made with this film, so we do not know the extent to which the observed permeation changes are reversible.

Table 1: Limiting Permeabilities for Ion Etched SiN_x Films

Etch Type	Over-etch Time (min)	No. of Membranes	Permeability ($mols^{-1}m^{-2}Pa^{-1}$)
Bosch	11	5	initially $< 4x10^{-11}$
Bosch	22	2	$< 2x10^{-11}$
Bosch	33	1	permeable @ $1x10^{-9}$
RIE	4	4	$< 7x10^{-11}$
RIE	8	6	permeable @ $1.6x10^{-8}$
RIE	12	6	$< 1x10^{-11}$

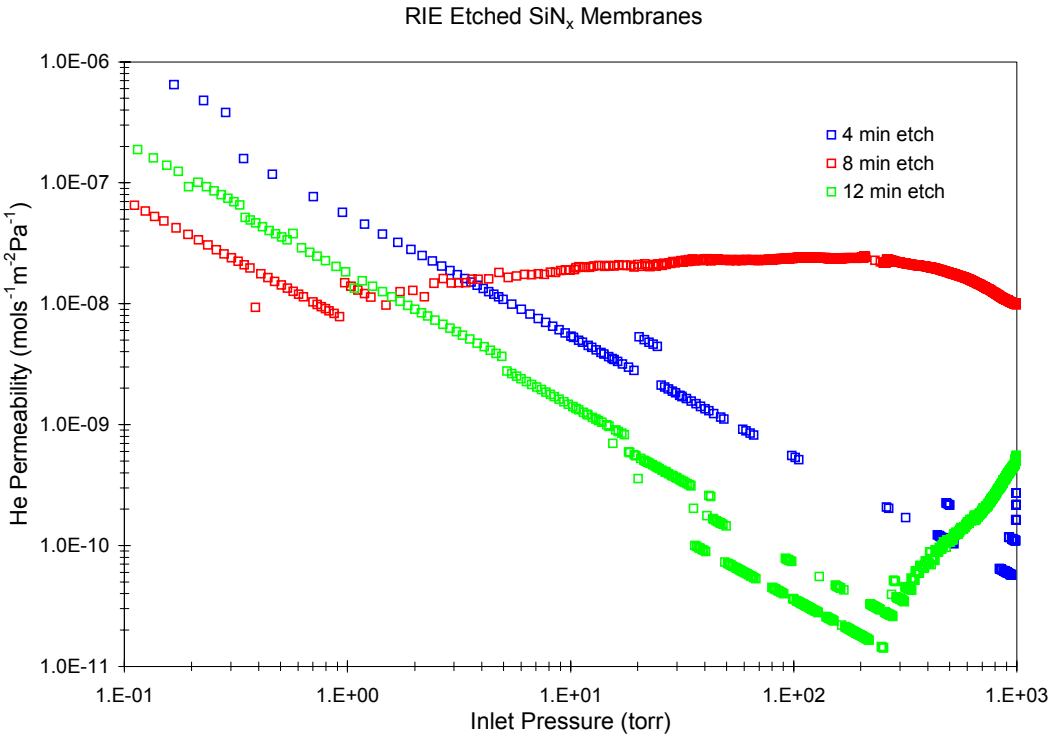

Figure 6. Variation in Bosch Etched SiN_x Film Permeability with Inlet Pressure

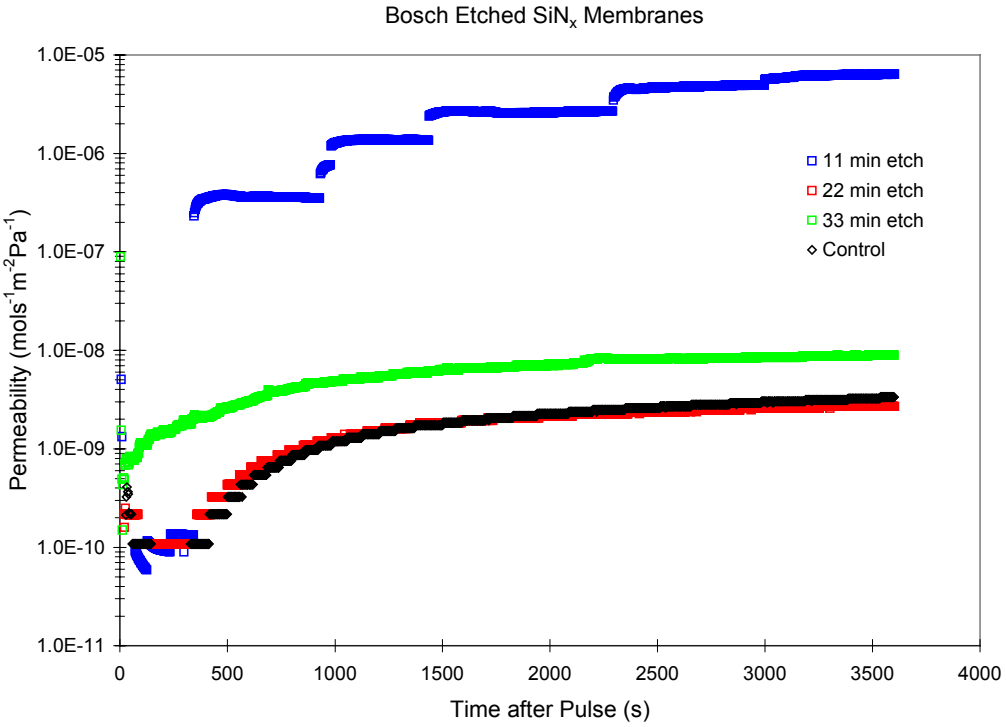

Figure 7: Time Variation in Bosch Etched SiN_x Films Permeability with a 1000 torr Pressure Pulse

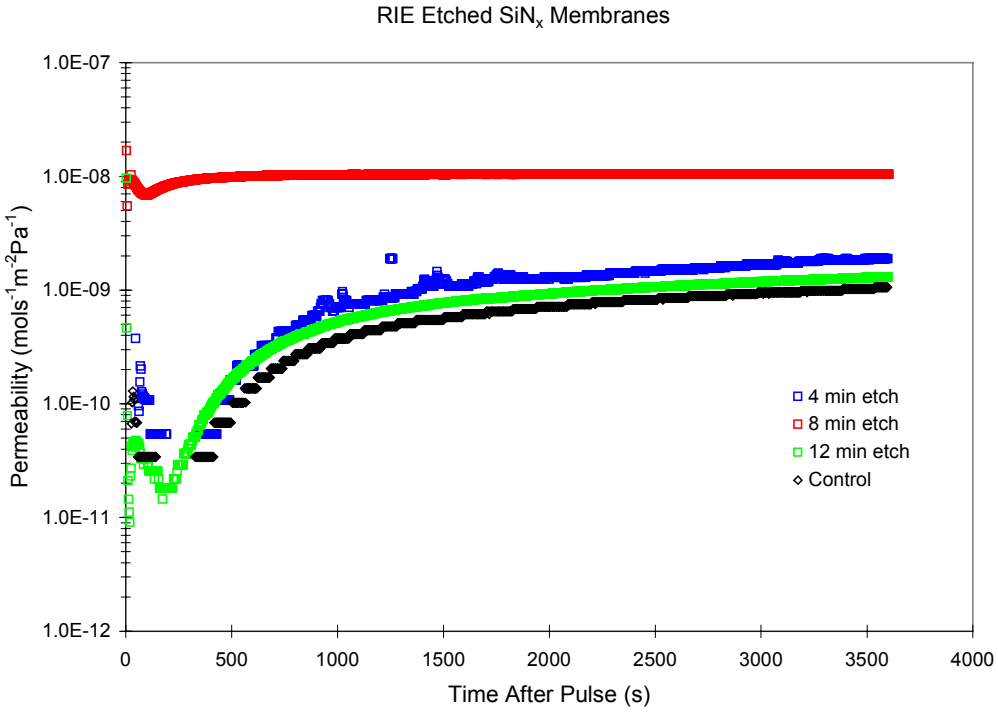

Figure 8: Time Variation in RIE Etched SiN_x Films Permeability with a 1000 torr Pressure Pulse

5. Discussion

We have demonstrated that the silicon nitride membranes produced using a Bosch etch followed by an RIE etch (8 min overetch) were permeable to gas but not liquid. This was shown in two separate experiments. One with water and one with helium. The membranes withstood approximately 25 *atm* of pressure without transporting water. A permeability of 1.6 x 10^{-8} $mol\ m^{-2}\ Pa^{-1}\ s^{-1}$ of helium was measured for membranes processed identically to those fabricated at the entrance and exit of microfluidic channels that were surface micromachined using silicon nitride. The measurement was made at the same scale as the microchannel using membranes processed in an identical manner (8 min. RIE overetch).

The results from the permeability measurements suggest that permeability was induced in the membrane films through the formation of microfractures. These fractures remain small with cross-sectional dimensions of less than 100 *nm* as evidenced by the presence of only molecular flow up to 1000 *Torr*.

The membranes can next be applied to the problem of controlling air bubbles in microfluidic liquid flows. Unwanted air bubbles can block liquid flows and break up liquid volumes that should remain intact. Controlled air bubble introduction and removal can be used to separate and mix chemical sample volumes in controlled on-chip chemical experiments.

As a simple bubble removal case, consider a channel completely open at the entrance with a silicon nitride membrane at one exit and an open second exit. A sample containing an unwanted air bubble is introduced at the entrance. The air bubble can be pushed to the exit containing the membrane and vented through the membrane. The air bubble can be removed without effecting the liquid volume which can now be routed out the fully open exit for further processing.

The number of moles vented per second can be calculated from the permeability test results. For a 200 μm diameter membrane under 10 *atm* of pressure, the leak rate (LR) is:

$$LR = \left(1.6\times10^{-8}\right)\cdot\left(1.01\times10^{6}\right)\cdot\left(3.1416\times10^{-8}\right) = 5\times10^{-10}\ mol/s$$

This calculation assumes that the entire area of the membrane is available for gas to leak through. The permeability calculation was made with the same assumption. As can be seen from Fig. 3 there is considerable variability in the surface topography and therefore also probably the permeability across the membrane. For most accurate results only the permeable area of the membrane should be considered when calculating permeability and leak rake. We are not sure what the permeable membrane area is so we used the full membrane area in our calculations.

An equivalent volume leak rate for air can be calculated using the ideal gas law with an adjustment to account for the molecular weight difference between air and helium.

$$\dot{V} = 0.45\times10^{-12}\ m^3/s = 0.45\ nl/s$$

This volume leak rate is equivalent to purging an air bubble approximately 200 μm x 2 μm x 1 *mm* in one second. Such a bubble could completely fill a typical microfluidic system. In order to fully implement a bubble control system we plan to fabricate and test a surface micromachined microfluidic system containing these membrane bubble vents. This microfluidic system might also be used to investigate the possibility of using the membranes as a gas separation system. We also plan to more fully investigate the phenomena of micro-crack formation that leads to membrane permeability.

Acknowledgement

Sandia is a multiprogram laboratory operated by Sandia Corporation, a Lockheed Martin Company, for the United States Department of Energy under Contract DE-AC04-94AL95000. We would like to thank the staff of the Microelectronics Development Laboratory for fabricating and releasing the silicon nitride channels, Daniel Gutierrez for assembling and testing channels containing membranes, and Mike J. Russell for performing the permeation measurements.

References

1. Bosch, Patent No. 5501893: *Method of Anisotropically Etching Silicon*. Robert Bosch GmbH., Issued 1996.
2. Brody, J. P., and P. Yager, "Low Reynolds Number Micro-Fluidic Devices", Solid-State Sensor and Actuator Workshop, Hilton Head Island, South Carolina,1996.
3. Cees J. M. van Rijn, G. J. Veldhuis and S. Kuiper, "Nanosieves with microsystem technology for microfiltration applications", Nanotechnology, vol. 9, pp. 343-345, 1998.
4. Chu, W-H, R. Chin, and T. Huen, "Silicon Membrane Nanofilters from Sacrificial Oxide Removal", Journal of MicroElectroMechanical Systems, vol. 8, no. 1, March 1999.
5. Eaton W. P., *Surface Micromachined Pressure Transducers*, PhD Dissertation, University of New Mexico, 1997.
6. Giddings J. C., "Field-Flow Fractionation: Analysis of Macromolecular, Colloidal, and Particulate Materials", Science, vol. 260, pp 1456-1465, 1993.
7. Harris J. D. and A. Van Den Berg, *Micro Total Analysis Systems*, Kluwer Academic Publishers, 1998.
8. Mulder M, *Basic Principles of Membrane Technology*, Kluwer Academic Publishers, 1996.
9. Roth A., *Vacuum Technology*, North-Holland, New York, 1982, p.112.
10. Sing K.S.W., D.H. Everett, R.A.W. Haul, L. Moscou, R. A. Pierotti, J. Rouquerol and T. Siemieniewska, Pure & Appl. Chem. 57(4), 1985, 603.
11. Steckelmacher W., Vacuum 28(6,7), 1978, 269.

12. Thomson S.L. and W.R. Owens, Vacuum 25, 1975, 151.
13. Wakeman, R. J., J. L. Henshall and S. G. NG, "SiAlON Membrane Coated silicon Nitride Microfilters", Chemical Engineering Research and Design, vol. 72, no. A2, pp. 227-235, 1994.
14. Yamamoto H. and S. Masuda, "Electrostatic Formation of Ceramic Membrane", Ceramic Transactions, pp. 305-314, 1993.
15. Yang X., J. M. Yang, X. Q. Wang, E. Meng, Y. C. Tai, and C. M. Ho, "Micromachined Membrane Particle Filters", MEMS 99, pp. 137-142, 1999.